

Received December 10, 2018, accepted December 24, 2018, date of publication January 7, 2019, date of current version January 23, 2019.

Digital Object Identifier 10.1109/ACCESS.2019.2890987

# Device-to-Device (D2D) Communication as a Bootstrapping System in a Wireless Cellular Network

NASREEN ANJUM<sup>1</sup>, ZHAOHUI YANG<sup>1</sup>, HADI SAKI<sup>1</sup>, MEHREEN KIRAN<sup>2</sup>,  
AND MOHAMMAD SHIKH-BAHAEI<sup>1</sup>, (Senior Member, IEEE)

<sup>1</sup>Department of Informatics, King's College London, London WC2B 4BG, U.K.

<sup>2</sup>Department of Computer Science, Institute of Management Sciences, Peshawar 25000, Pakistan

Corresponding author: Nasreen Anjum (nasreen.anjum@kcl.ac.uk)

This work was supported in part by the Engineering and Physical Sciences Research Council under Grant EP/P022723/1, and in part by the Schlumberger Faculty for Future Fellowship Program.

**ABSTRACT** Device-to-Device (D2D) communication is considered to be a promising form of technology to distribute video contents to nearby users and devices at a high data rate and with few delays. In this paper, we propose utilizing the D2D services and cache of mobile devices as a bootstrapping system in a cellular network. The main objective of a bootstrapping-D2D (BD2D) system is to improve the quality of service in terms of achieving the minimum startup-time of popular video files in a cellular network. To achieve our objective, we propose a new caching concept for D2D communication in which each mobile device can cache and share the initial video portion or initial segments of the popular video files to other proximate users via a D2D communication link. We formulate an optimization problem that maximizes the cache-hit ratio of initial segments of the most popular video contents. The basic aim is to move the initial segments as close as possible to the wireless users. We also propose a network-assisted D2D architecture called mobile content delivery network-assisted-BD2D and algorithms that assist the BD2D system in the discovery of devices that have cached the initial segments of the requested video files, in cache placement decisions, and also in the registration of potential D2D devices at the core network. We evaluate the performance of the BD2D system and propose algorithms through extensive simulations under real wireless network conditions, such as interference, fading, and shadowing. Our concluding simulation results demonstrate that bootstrapping the initial segments using the short range BD2D system can significantly reduce the average startup-time of video files in comparison with bootstrapping the initial segments from the traditional cellular system.

**INDEX TERMS** Device-to-Device (D2D), startup-time, wireless cellular networks, mobile content delivery network (MCDN), quality-of-service (QoS), delay, cache-hit.

## I. INTRODUCTION

Driven by clients' growing appetite for videos, we are currently seeing huge growth in video data traffic over cellular networks. According to the latest Cisco Visual Networking Index update [1], mobile data traffic is expected to grow by up to 49 exabytes per month by 2021 and, 75% of the total global video traffic will be generated by smart handheld devices. The resulting phenomenal growth in mobile video traffic over cellular communication has created opportunities for wireless service providers (WSPs) to maximize their number of customers and business revenue. However, to achieve that, WSPs need to keep their customers

satisfied by providing high quality services such as low video *startup-time*.<sup>1</sup>

A number of online studies have reported that a longer *startup-time* may cause users to abandon videos soon after starting to watch them. For instance, one study suggested that viewers of online videos follow the "two-second rule" [2], [3], meaning that they are more likely to abandon a video if it does not start within two seconds. It also means they are less likely to return to the website. More specifically,

<sup>1</sup>We define *startup-time* to be the total waiting time that the mobile user spends waiting until the first frame of video is played on her/his display screen.

studies have suggested that viewers of short length videos are less tolerant of slow *startup-time* compared to those who watch longer videos. For businesses, one extra second of delay on a web video can cause millions of dollars of lost sales revenue. Therefore, providing a high quality service (QoS) for cellular users where videos start quickly is one of the major goals of mobile network operators (MNOs) [4], [5].

Unfortunately, due to a scarcity of radio resources [6]–[10] and inherent adverse features such as channel fading, interference, and variable end-to-end delay [11], cellular infrastructure (3G/4G)<sup>2</sup> is failing to meet customer expectations, and Video on Demand (VoD) streaming is plagued by hundreds of milliseconds of delay when users stream video through the base station (BS) [12]. To deal with these issues, one of the best-known strategies adopted by the MNOs is to increase the density of the currently deployed wireless infrastructure [13]. This is achieved either by deploying very dense BS antennas in the form of “massive MIMO (Multiple Input and Multiple Output)”, or by deploying “dense but small cells”, resulting in the mobile back-haul network becoming a bottleneck. The deployment of high-speed fiber-optic cable is expensive and requires a higher CAPEX (CAPEX) and Operating EXPenditure (OPEX) [14]. Meanwhile, the majority of mobile data users expect and demand high quality data services, however, at the same time they are not willing to pay for mobile data usage and services offered by their operators. Now, the prodigious interest of MNOs and the research community (**and also the main objective of this article**) is to find alternative and efficient methods that mitigate the stress of the core network and improve the QoS in terms of reducing the video *startup-time* without requiring any additional CAPEX and OPEX.

Recently, D2D communication has become an attractive distributed computing paradigm, following the popularity and standardization of unlicensed band D2D protocols in Long-Term Evolution (LTE) Rel.12 [12]. Device-to-Device technology supports direct communication between devices located in close proximity to high bit-rates and low delay without requiring the traversal through a BS [15], [16]. Some initial case studies have investigated the impact of video distribution via D2D on cellular networks and suggested employing D2D technology to assist the BS in distributing multimedia content. For instance, Ji *et al.* [17] proposed deterministic and random caching policies for the D2D caching network from an information theory perspective, that may achieve the upper bound within a constant multiplicative. The authors in [18] proposed a novel architecture to investigate the throughput gain from a D2D caching system. The simulation results show that their proposal for video dissemination through D2D communication can enhance the video throughput by two orders of magnitude. Another study [19] proposed an algorithm to cache and distribute an Online Social Network’s (OSN) multimedia content through D2D communication by exploiting the characteristics of

social networks. The simulation results reported an increase in the supported data rate of the system. To increase the probability of successful content delivery, Malak *et al.* [20] proposed a new caching technique for D2D communication, derived from the results of stochastic geometry in the presence of noise and interference. An optimization problem is formulated based on the Zipf distribution to determine the optimal cache probability that can maximize the number of requests satisfied for the desired video content using the D2D communication links. Similarly, Zhang *et al.* [21] formulated an optimization problem to maximize the throughput of the system by taking into consideration the transmission power constraints. Their proposal for D2D caching in combination with transmission power allocation constraints has led to an improvement in system throughput.

All the aforementioned research efforts have focused on improving the overall system throughput and have exploited the most common caching strategy in which complete and the most popular video content is cached on the users’ limited storage space. Moreover, all mobile devices are assumed to be rich in storage capacity. However, in reality mobile devices are highly heterogeneous in resources. Although storage space on wireless devices is increasing, they have heterogeneous and limited cache capacities. Furthermore, the size and popularity of video files are also highly dynamic and mobile devices can sometimes cache and share only a fraction of the video file [22]. Therefore, considering a large video file as a whole and a single cache unit on the users’ storage space is inefficient.

As our first contribution, unlike prior D2D caching proposals, we propose a new D2D caching concept called “*D2D communication as a bootstrapping system*<sup>3</sup> in a wireless cellular network”. The BD2D system allows mobile devices to cache and share only the initial-segments<sup>4</sup> via a D2D communication link to static or semi-static cellular users. Our simulation results show that the BD2D approach can significantly reduce the video *startup-time* in comparison to bootstrapping the initial-segments from the BS. To the best of our knowledge, we presented a detailed analysis of a D2D caching system as a bootstrapping system in a cellular network for the first time.

The first step before initiating a D2D communication between the two proximity devices is that they must detect the presence of each other within their radio frequency range. The device discovery procedure can be accomplished autonomously through the (occasional or periodical) broadcast of the proximity detection signal (PDS) also referred to as beacon signal. However, there can be a situation when a

<sup>3</sup>The bootstrapping term is used in typical peer-to-peer (P2P) and peer-assisted content delivery networks (PA-CDNs) to represent nodes that provide initial-segments to the requesting device to achieve a low *startup-time* [23], [24].

<sup>4</sup>In this paper, for brevity, we use the term initial-segments to represent the initial portion of the video files. For example, initial-segments containing a 10-second video clip. The video file is sliced into smaller segments before it is transmitted to the end-user and is manipulated as a minimum unit for caching and transmitting the popular video files.

<sup>2</sup>3rd Generation/4th Generation

device periodically transmits beacon signals in order to find the potential D2D candidate, but no potential D2D device is available in close proximity. In such a situation, a D2D communication system may experience longer startup delays resulting in poor QoS for video streaming services. Therefore, to achieve a good QoS better control over the D2D communication system is mandatory.

As for our second contribution, we introduce a novel network-assisted D2D architecture<sup>5</sup> called a M-BD2D (Mobile Content Delivery Network (MCDN) assisted-BD2D) system that assists the BD2D system in the discovery of devices that have cached the initial-segments of the requested video files, in cache placement decisions, and also in the registration of D2D devices at the core network.

There is a lack of research effort describing the network-assisted D2D architecture that provides support and assistance in carrying out basic D2D procedures such as device discovery, connection establishment and mode selection etc. The idea of augmenting the D2D capabilities into an LTE-Advanced architecture is first proposed in [25]. In this architecture, Packet Data Network Gateway (PDN-G)<sup>6</sup> assists the D2D network in a device discovery and connection establishment. Moreover, the eNodeB is supposed to have full control over the spectrum resources used by the cellular and the D2D users. In order to minimize the effects of interference between cellular and D2D users, eNodeB can optimize the transmission power of D2D users by utilizing the cellular power control information of potential D2D devices. Yang *et al.* [26] introduce a Proximity Service Control Function (PSCF) in the PDN-G that can detect the potential traffic flow and find the pairs of devices that are linked through the same flow. Based on an observation that the eNodeB is an anchor point between the UEs and Evolved Packet Core (EPC) and can track the UEs positions in their active mode, Agarwal *et al.* [27] propose the integration of D2D capabilities such as device discovery and authentication and security in the eNodeB. They also propose some protocol modifications in the LTE standard to embed the authorization and authentication procedure for the D2D communication to occur. Raghathan *et al.* [28] propose adding a new network entity called *D2D-server*. The *D2D-server* is placed within or outside the EPC architecture. In a case when a *D2D-server* is placed outside the EPC, it is supposed to have a direct interface with other logical network entities such as Mobility Management Entity (MME). The *D2D-server* is responsible for handling some important functions such as the device registration process, connection establishment, tracking the locations of D2D devices and service information requested or offered by the D2D users. Similarly,

<sup>5</sup>The major difference between a traditional D2D system and a network-assisted D2D system lies in the support from the backbone system: the former is a self-supported independent system, while the latter uses assistance from the network in device discovery, connection establishment, mode selection and power management etc.

<sup>6</sup>The PDN-G allocates IP addresses to the UEs. It keeps and maintains a routing table to route the traffic from/to the Internet. It also routes the traffic to the proper eNodeB serving the UEs.

Pyattaev *et al.* [29] propose the introduction of a few network entities in the 3GPP architecture that can assist in device discovery and service continuity.

In the context of the aforementioned discussion, our proposed architecture is different from the approaches proposed in the literature. The M-BD2D exploits the services of a MCDN<sup>7</sup> [30], [31] to assist the BD2D system. Similar to CDN,<sup>8</sup> MCDN exploits caching and prefetching techniques in order to optimize the bandwidth resources and reduces the latency by shifting the content from the overloaded content providers to the proxies or caches located closer to the content consumers. Our proposed M-BD2D system is an integral element of 3rd Generation Partnership Project (3GPP) LTE-Advanced architecture and relies on servers deployed within the Serving Point Gateway (SGW) and PDN-G which are internally connected to each other.

Further, we have formulated an optimization solution that maximizes the cache-hit ratio of initial-segments of requested video content and allows the mobile devices to find and download the initial-segments from the devices at a very short distance and with low startup download time. We have used a system model in which mobile devices are not limited to establishing a D2D connection within a cluster. In fact, a mobile device can establish a D2D connection with a neighboring device that falls within the transmission range. For further clarity, our contributions in this article are summarized as follows:

- We propose a new caching concept called a BD2D system that allows the D2D devices in a cellular network to cache and share only the beginning fragment of the most popular videos files with devices in close proximity, and with a low startup download time.
- We propose a novel network-assisted D2D architecture that exploits the services of MCDN and assists the BD2D caching system in the discovery of devices that have cached the initial-segments of the requested video files, in cache placement decisions, and also in the registration process of D2D devices at the core network.
- We have formulated an optimization solution that maximizes the cache-hit ratio of initial-segments of the most popular video files. To solve this nonconvex cache-hit ratio maximization problem, an iterative algorithm is proposed, where the closed-form cache probability is obtained in each step. Our simulation results demonstrate that the BD2D caching system can achieve better performance in terms of a higher percentage of cache-hit ratio (i.e., from 95% to 100%) even with small storage space.
- We consider several realistic assumptions in our simulations to analyze the performance of a BD2D sys-

<sup>7</sup>MNOs have now started to integrate the CDN capabilities in the existing 3GPP LTE-A architecture. Such MNO-owned CDNs are referred to as Mobile-CDN (MCDN).

<sup>8</sup>Content Delivery Network (CDN) is a system of servers that distribute content to users from the nearest geographically deployed edge nodes/servers with low latency and high QoS.

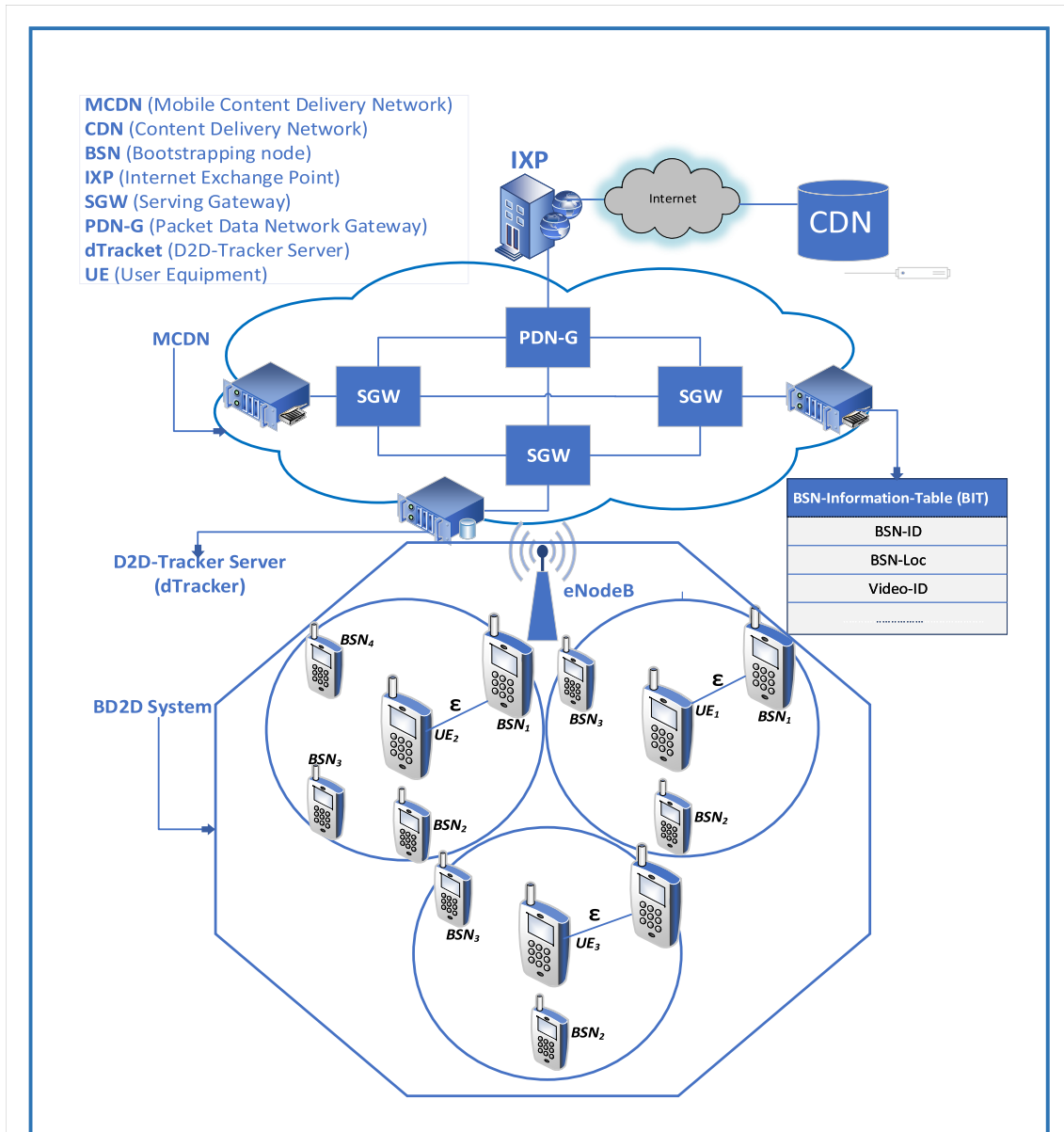


FIGURE 1. System Architecture of M-BD2D.

tem: (i) a realistic channel model for the D2D communication system that is based on an indoor office environment with the well-known standard WINNER II channel model [32], [33], (ii) consider the important wireless link characteristics such as interference, path loss and body shadowing parameters for both Line-of-Sight (LOS) and Non-Line-of-Sight (NLOS) scenarios.

The remainder of this paper is organized as follows: Section II describes our new caching concept and the architecture of a M-BD2D system. Section III presents the system model and the derived optimization problem. Simulation results are discussed and analyzed in section IV, and the conclusions are drawn in section V.

## II. M-BD2D ARCHITECTURE

In this section, we first describe the M-BD2D architecture along with its components. Then, system operation is discussed in detail. As shown in Fig. 1, M-BD2D architecture comprises two major components: BD2D and MCDN.

### A. BD2D SYSTEM

The BD2D system consists of BSNs (BootStrapping Nodes) and UEs (User Equipments). The BSN is a mobile device that can cache the initial-segments of the most popular video files and share them upon request using D2D opportunities. We term this act of sharing initial video segments from a D2D link as BD2D. The BSN can retrieve and play the desired

videos from its own storage with zero *startup-time*. A UE in our BD2D system is a cellular device that requests the video content and directly receives the initial-segment from the closest BSN or eNodeB depending on the channel quality and the corresponding link rate. Thus, instead of relying on the core of the cellular network, a UE can retrieve the initial-segments of desired video files from the neighboring short-range caches.

### 1) BD2D CACHING SYSTEM

We assume that a video file in the BD2D system is composed of a number of small and equal size video segments. Each segment is a group of pictures called a frame. The first segment which contains a short video clip, will be referred to as an initial-segment and is the basic unit of operation. A BSN in our video streaming system maintains a playback buffer that stores all received segments from the network or neighboring BSNs. The received segments from different sources are assembled in the playback buffer in a playback order. The media player of a mobile device displays the content from this buffer. For simplicity, we assume that all video files are encoded using a constant bit-rate (CBR) encoding technique.

In caching systems of fixed line networks such as peer-assisted content delivery networks (PA-CDNs) and peer-to-peer (P2P) systems, cache locations and cache topology are fixed. The cache placement decisions and coordination between the caches can be predicted and determined by solving the analytical model and by using prior knowledge of the cache demands and the cache structure. However, in the D2D-cache networks due to mobility the location and topology of devices is not fixed. In such cases, it is very difficult and complicated to figure out the optimal object placement. However, the popularity of video objects can be predicted from historical statistics. Many studies have reported a skewed distribution of users' interest towards a small fraction of top ranked content [34]. We prefer to use the Zipf distribution model which has been used in many studies for the analysis of D2D caching [35], [36]. We assume that each cellular user from a cell independently and randomly requests a file  $j$  from the library of size  $\mathcal{N}$ , and the popularity of files can be expressed as:

$$\mathcal{F}_j = \frac{j^{-\gamma_r}}{\sum_{\ell=1}^{\mathcal{N}} \frac{1}{\ell^{\gamma_r}}}, \quad 1 \leq j \leq \mathcal{N} \quad (1)$$

where  $\gamma_r$  is a value of the exponent characterizing the distribution i.e., larger the value of  $\gamma_r$ , more popular files are demanded; and  $\mathcal{N}$  is the number of video contents in the library. We consider a caching strategy, in which BSNs will only cache the initial-segments of video content with a Zipf exponent  $\gamma_c$ , determined by the network administrator. Therefore, a cache-decision is made for each request for content. In such a case, the initial video segments of the most popular video content will be cached and delivered through the BD2D caching system.

### 2) BD2D OPERATING MODE

To guarantee the QoS D2D link, the BD2D system will operate in a dedicated/orthogonal mode [37], [38]. This means that the BD2D system will exploit the dedicated spectrum of resources of the network to share the initial-video clips with the neighboring devices in the cellular network, while the remaining video segments will be delivered using a traditional cellular mode via eNodeB. We suggested the use of a dedicated/orthogonal mode for the BD2D system because it guarantees the QoS in comparison to reuse (or underlay) mode. In underlay sharing mode, D2D devices share the cellular spectrum of resources with the cellular users.

The dedicated sharing mode allows D2D devices to establish a direct link without causing any horrendous interference to cellular users with optimum significant performance (however, interference caused by D2D transmitters at the receiver end will exist).

### B. MCDN ARCHITECTURE

The 3GPP LTE-Advanced architecture is characterized as a fully centralized radio access network in which PDN-G acts as an anchor point between the UEs and the external networks such as Internet and private networks. When a UE requests for some video content, the IP traffic generated by the UE is force to traverse through the core network all way from the SGW to the PDN-G by means of a tunneling procedure. In contrast, when a user requests some multimedia content in a MCDN, his/her request is redirected to the closest edge node/server via the eNodeB. The edge nodes/servers are deployed within the EPC architecture such as along the SGW or PDN-G [30], [31] to integrate the CDN capabilities within the existing 3GPP LTE-Advanced architecture. All edge nodes along the gateways jointly cache the most popular video content. This allows cellular users to find and download the content within the domain from the server geographically nearby. The edge nodes are directly connected to the SGWs and SGWs are connected to a set of BSs which provide wireless connectivity to the mobile devices. Liebsch and Yousaf [39] have already investigated the direct connection between SGWs and their servers. SGW provides a wide variety of critical functions for the 4G mobile core network. It forwards and routes packets to and from the eNodeB and PDN-G. By means of such a setup, servers deployed within the SGW can play an active and crucial role in device discovery, mode selection, service continuity, D2D-indexing and cache placement decisions. However, in our architecture servers deployed within the SGW play three important roles: (a) actual media streaming server (*MSS*), (b) D2D-Tracker server (*dTracker*) and (c) cache-decision manager (*CDM*).

To distribute and deliver the requested video files from the closest server, as a *MSS*, it will cache the most popular video files. As a *dTracker*, it will maintain and manage a lookup table of registered BSNs and acts as a relay between UEs as well as a network for content exchange. We call this table a BSN-Information Table (BIT) and will include an

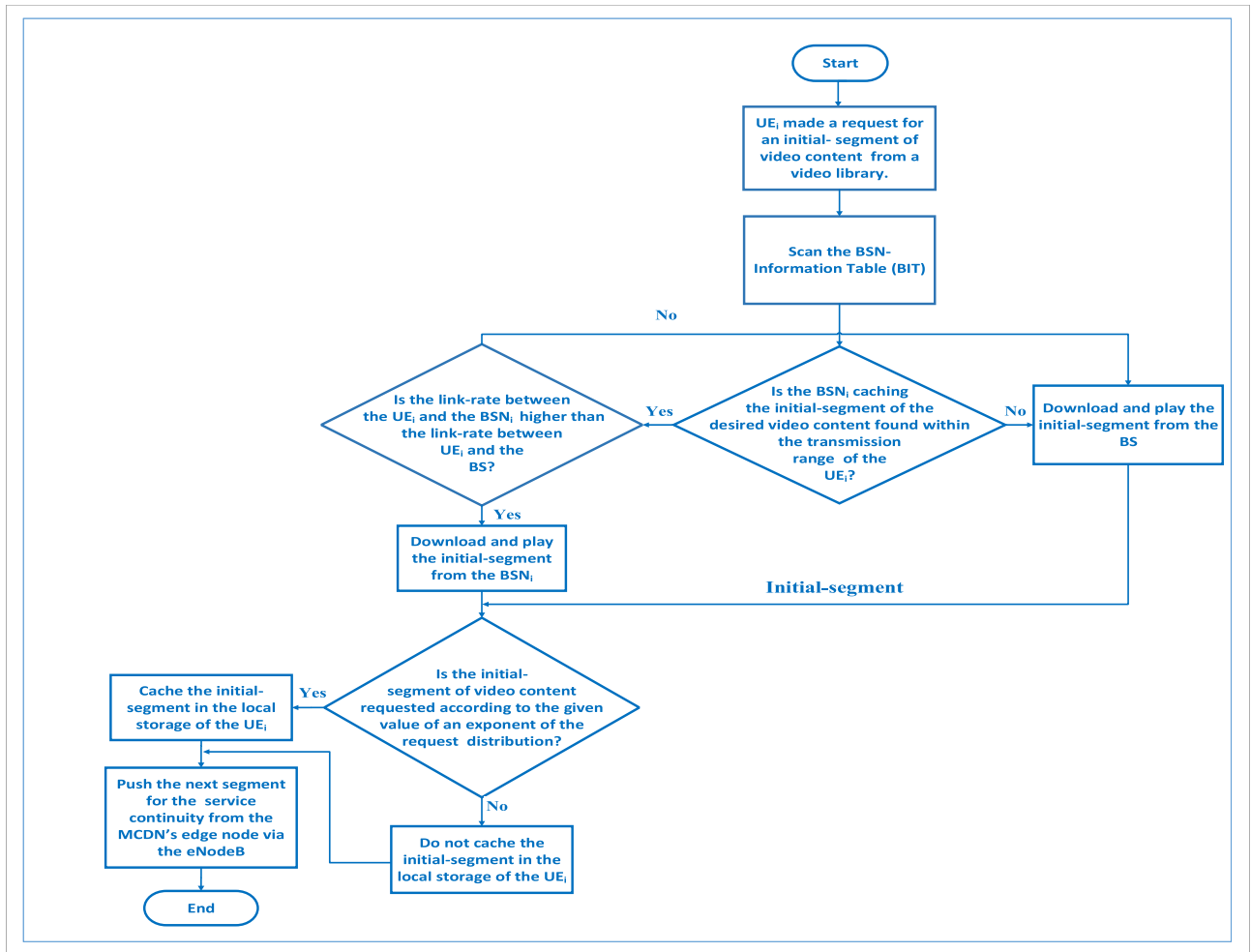


FIGURE 2. The flowchart of the delivery of the initial-segments through the M-BD2D system.

entry for each BSN including the BSN-ID, video-ID, and their locations in a cell using the available positioning services. The *dTracker* in M-BD2D architecture will constantly update the BIT information by communicating with available positioning services to keep track of BSN locations and the content they have cached. For instance, eNodeB might assist in tracking and updating the locations of mobile devices. This information will be used by the *dTracker* to choose the appropriate BSN and then send this information to the requesting UE to establish a connection with the BSN and then download the initial-segments of the desired video file.

As a CDM, it will handle the most important cache problem, i.e., how to cache, which means initial-segments of which content will be cached in a local cache of each BSN.

### C. SYSTEM OPERATION, CACHING ALGORITHM AND REGISTRATION PROCESS

The workflow in M-BD2D architecture is shown in Fig. 2 and for more detail see Algorithm 1. At the beginning there is no BSN. When a user clicks on the content link provided by the content providers (CPs) such as BBC iPlayer or Netflix,

for some video content the mobile network relays the user request from the BS to the SGW. Upon receiving requests for the content, the SGW will first check whether the video is available in its own local storage. If yes, the requested video is delivered directly via the BS to the requesting device; otherwise it will look for the video (possibly through a directory service) from local servers of other SGWs. If no copy is found in the network of streaming edge servers, the request is relayed to the external Internet via a PDN-G.

Once the UE has received the initial-segments along with the cache's decision, it will store the segments in its local storage and the *dTracker* will register the requesting UE as a BSN using its ID, current location and video-ID into the BIT. With the creation of BIT, the SGW can assign the task of delivering initial-segments to the BSNs. If the storage of a BSN is full, the new initial-segment will be replaced using some optimal cache replacement algorithm such as a least recently used (LRU) algorithm.

When the SGW receives the request for the video content, to provide the initial-segments from a D2D link it will filter the information stored in the BIT to find the BSN within the

**Algorithm 1** Initial-segment placement Algorithm in the BD2D system

- 1: **for all** requests for the initial-segment of video content of index  $j$  from a library of size  $\mathcal{N}$  **do**,
- 2:   **if** the size of the initial-segment of the requested video content of index  $j$  is less than the storage capacity  $\mathcal{C}$  of the requesting mobile device and has been requested according to the specified request distribution's exponent value i.e.,  $\gamma_r$  **then**,
- 3:     download, play and cache the initial-segment in the storage of a requesting mobile device.
- 4:   **else**
- 5:     download and play the initial-segment but do not cache in the storage of a requesting mobile device.
- 6:   **end if**
- 7: **end for**

proximity of the requesting UE that has cached the initial-segments of the desired video content. Since achieving a quicker *startup-time* in a cellular network is our prime concern, channel state information (CSI) of each communication link is required to select the best mode for delivering the initial video clip. Based on the quality of the channel and other link-related information such as interference, the most appropriate operating mode is selected.

Similar to some of the network-assisted D2D systems such as [29] and [40], eNodeB in M-BD2D system is actively involved in collecting statistics about the channel conditions and inter cell interference etc. Our M-BD2D system uses the method prescribed in [29] and [41] to acquire the full CSI and based on that will select the most suitable mode for the D2D communication. If the channel quality between the UE and the BSN is better than the channel quality between UE and eNB, then UE will be asked to establish a connection and download the initial-segments from the corresponding BSN. Meanwhile, SGW will forward the next video segments via eNodeB to the buffer of the UE for the sake of service continuity.

In the presence of multiple requests or a flash crowd, the M-BD2D will accept or reject the users' requests for the initial-segments of the desired video content according to the rules specified in the admission control system. Different admission control policies may be designed as per the requirements of the system. For example, the system may process the users' requests based on the channel conditions. However, this is beyond the scope of this paper.

**III. SYSTEM MODEL AND PROBLEM FORMULATION**

Our main objective in this article is to minimize the average *startup-time* of on-demand video streaming applications in a cellular network using D2D opportunities and the cache capacity of mobile devices. We solve the corresponding problem by formulating the optimization problem that maximizes the cache-hit probability of initial-segments of the most popular video content at each BSN. The main idea is to move

**TABLE 1.** Parameters of initial-segment placement problem (IPP).

Variable	Description
$\lambda_\eta$	Density distribution of BSNs
$\mathcal{N}$	Number of video files
$\mathcal{M}$	Number of requests or UEs in a cell
$\epsilon_{max}$	Maximum transmission range of wireless nodes (UEs and BSNs)
$\mathcal{S}_j$	Size of an initial-segment of a video content $j$
$\mathcal{C}$	Cache capacity
$\mathcal{F}^{(i,j)}$	Request probability of an initial-segment of a video content $j$
$p^{(i,j)}$	Cache probability of an initial-segment of a video content $j$ at requesting UE $_i$
$\mathcal{P}_H^{(i,j)}(\epsilon_{max})$	Cache-hit probability of an initial-segment of a video content $j$ at UE $_i$
$\mathcal{P}_M^{(i,j)}$	Cache-miss probability of an initial-segment of a video content $j$ at UE $_i$

the initial-segments closer to the cellular users. We called our optimization problem the **initial-segment placement problem (IPP)**.

In this section, we first describe our system model. Then, IPP is formulated and its solution is derived. The parameters we used in IPP formulation are given in Table 1.

**A. SYSTEM MODEL**

For simplicity and without the loss of generality, we consider a cellular network where a BS can serve only one cell (see Fig. 1). We assume that, an  $\eta$  number of BSNs are distributed across the cell according to a Poisson Point Process (PPP) with an intensity  $\lambda_\eta$ . Let a UE $_i$  (for  $i = 1, \dots, \mathcal{M}$ ) generates a request from an arbitrary position for an initial-segment of a video content  $j$ . The probability that  $\eta$  number of BSNs present within a distance  $\epsilon$  from the requesting UE $_i$  is given as

$$\mathcal{P}_\eta(\epsilon) = \frac{e^{-\lambda\pi\epsilon^2}}{\eta!} (\lambda\pi\epsilon^2)^\eta. \tag{2}$$

To achieve the maximum cache-hit ratio, each BSN will cache the initial-segments of video content of index  $j$  from a library of size  $\mathcal{N}$  subject to the availability of cache space. Each initial-segment will be cached at the requested UE $_i$  according to the cache probability  $p^{(i,j)}$ . For the sake of tractability, we assume that the size of the initial-segment is fixed and given by  $\mathcal{S}_j = \mathcal{D}_t \times \beta$ , where  $\mathcal{D}_t$  is the size of an initial-segment in MB and  $\beta$  is the bit-rate in Mbps. Since each initial-segment will be cached independently with cache probability  $p^{(i,j)}$ , therefore, according to the thinning property of the PPP each initial-segment will be disseminated with intensity  $\lambda p^{(i,j)}$  in a cell.

We define the initial-segment cache-hit as an event in which a UE $_i$  requests for an initial-segment of video content  $j$  and finds at least one BSN within its maximum transmission range  $\epsilon_{max}$ . The probability that UE $_i$  can find an initial-segment of requested content  $j$  within its fixed maximum transmission range  $\epsilon_{max}$  is given as:

$$\mathcal{P}_H^{(i,j)}(\epsilon_{max}) = 1 - \mathcal{P}_M^{(i,j)} = 1 - e^{-\lambda p^{(i,j)} \pi \epsilon_{max}^2}, \tag{3}$$

where  $P_M^{(i,j)}$  is the probability of cache-miss, i.e., it indicates the situation when there exists no BSN within the transmission range of UE<sub>i</sub> caching the initial-segment of the requested video file (i.e., when  $\eta = 0$ ).

**B. PROBLEM FORMULATION**

We aim to minimize the average *startup-time* of on-demand streaming applications in a cellular network by achieving a maximum cache-hit ratio of initial-segments when each BSN has cached a subset of initial-segments, subject to the availability of storage. Let the caching capacity of each BSN be denoted by  $\mathcal{C}$ , which determines the total number of initial-segments that can be cached in the storage of a BSN. Let  $\mathcal{F}_{(i,j)}$  denote the request probability for the initial-segment of content  $j$  by an UE<sub>i</sub>. Now, our optimization problem can be formulated as:

$$\text{maximise}_{S_j, p_{(i,j)}} \sum_{i=1}^{\mathcal{M}} \sum_{j=1}^{\mathcal{N}} (1 - e^{-\lambda p_{(i,j)} \pi \epsilon_{max}^2}) \mathcal{F}_{(i,j)} S_j \quad (4)$$

$$\text{subject to} \sum_{j=1}^{\mathcal{N}} p_{(i,j)} S_j \leq \mathcal{C}, \quad i = 1, 2, \dots, \mathcal{M} \quad (5)$$

$$S_j \geq 0, \quad i = j = 1, 2, \dots, \mathcal{N} \quad (6)$$

$$0 \leq p_{(i,j)} \leq 1, \quad i = 1, 2, \dots, \mathcal{M}, \quad j = 1, 2, \dots, \mathcal{N}. \quad (7)$$

Our IPP is a cache-hit ratio maximization problem. The objective function (4) represents the cache-hit ratio of initial-segments. Constraint (5) represents the maximal cache capacity of each BSN. Through analyzing (4)-(7), the proposed IPP problem is a nonconvex problem with respect to  $S_j$  and  $p_{(i,j)}$ . It is generally difficult to achieve the global optimal solution to the nonconvex problem. In the following, we propose an iterative algorithm to obtain a suboptimal solution to the IPP problem (4)-(7) via alternatively optimizing  $p_{(i,j)}$  with fixed  $S_j$  and updating  $S_j$  with optimised  $p_{(i,j)}$ .

In the first step, we optimise cache probability  $p_{(i,j)}$  with fixed segment size  $S_j$ . Since the IPP problem (4)-(7) is a convex problem with fixed  $S_j$ , we consider the Karush-Kuhn-Tucker (KKT) conditions. The Lagrangian function of the IPP problem (4)-(7) with fixed  $S_j$  is given by

$$L(p_{(i,j)}, \alpha_i) = \sum_{i=1}^{\mathcal{M}} \sum_{j=1}^{\mathcal{N}} (1 - e^{-\lambda p_{(i,j)} \pi \epsilon_{max}^2}) \mathcal{F}_{(i,j)} S_j + \sum_{i=1}^{\mathcal{M}} \alpha_i (\mathcal{C} - \sum_{j=1}^{\mathcal{N}} p_{(i,j)}), \quad (8)$$

where  $\alpha_i$  is a non-negative Lagrangian multiplier associated with constraint (5). Thus,

$$\frac{\partial L}{\partial p_{(i,j)}} = \lambda \pi \epsilon_{max}^2 \mathcal{F}_{(i,j)} S_j e^{-\lambda p_{(i,j)} \pi \epsilon_{max}^2} - \alpha_i S_j. \quad (9)$$

Setting  $\frac{\partial L}{\partial p_{(i,j)}} = 0$ , we have

$$p_{(i,j)} = -\frac{1}{\lambda \pi \epsilon_{max}^2} \ln \frac{\alpha_i}{\lambda \pi \epsilon_{max}^2 \mathcal{F}_{(i,j)}}. \quad (10)$$

Combining (7) and (10), the value of  $p_{(i,j)}$  is given by

$$p_{(i,j)} = \left[ -\frac{1}{\lambda \pi \epsilon_{max}^2} \ln \frac{\alpha_i}{\lambda \pi \epsilon_{max}^2 \mathcal{F}_{(i,j)}} \right]_0^1, \quad (11)$$

where  $[a]_b^c = \min\{\max\{a, b\}, c\}$ .

According to (9) and  $\frac{\partial L}{\partial p_{(i,j)}} = 0$ , we have  $\alpha_i > 0$ . Therefore, the complementary slackness condition yields

$$\sum_{j=1}^{\mathcal{N}} p_{(i,j)} = \mathcal{C}. \quad (12)$$

Substituting (11) into (12), we have

$$\sum_{j=1}^{\mathcal{N}} \left[ -\frac{1}{\lambda \pi \epsilon_{max}^2} \ln \frac{\alpha_i}{\lambda \pi \epsilon_{max}^2 \mathcal{F}_{(i,j)}} \right]_0^1 S_j = \mathcal{C}. \quad (13)$$

Since the left-hand side of equation (13) is a monotonically decreasing function of  $\alpha_i$ , the value of  $\alpha_i$  satisfying equation (13) can be effectively obtained via the bisection method. Having obtained the value of Lagrange multiplier  $\alpha_i$ , we can calculate the optimal cache probability  $p_{(i,j)}$  of an initial-segment as in equation (11).

In the second step, we optimise segment size  $S_j$  with given cache probability  $p_{(i,j)}$  obtained in the previous step. The IPP problem (4)-(7) is a convex problem with fixed  $p_{(i,j)}$  is a liner problem, which can be effectively solved via the popular simplex method.

As a result, the iterative algorithm for solving the IPP problem (4)-(7) is given in Algorithm 2.

**Algorithm 2** : Iterative Algorithm

- 1: Initialise  $S_j^{(0)}, p_{(i,j)}^{(0)}$  and  $l = 0$ .
- 2: **repeat**
- 3: With given segment size  $S_j^{(l)}$ , obtain the optimal  $p_{(i,j)}^{(l+1)}$  of the IPP problem according to (11) and (13).
- 4: With given cache probability  $p_{(i,j)}^{(l+1)}$ , obtain the optimal  $S_j^{(l+1)}$  of the IPP problem by using the simplex method.
- 5: Set  $l = l + 1$ .
- 6: **until** Convergence

However, in order to avoid complexity we solve our optimization problem numerically using Monte Carlo simulations which asymptotically converges to the correct probability after 1000 Monte Carlo iterations.

**IV. PERFORMANCE EVALUATION**

This section provides a detailed discussion on simulation results in which we studied the performance of the BD2D approach. We divided our simulation experiments into two different sets, i.e., simulation results-I and simulation results-II. The first set of simulations find the optimal initial-segment size, i.e.,  $S_{opt}$ , and an exponent of caching distribution i.e.,  $\gamma_c$ , that maximizes the average cache-hit ratio of initial-segments



**TABLE 2.** Simulation parameters of first set of simulations.

Parameters	Value
$\epsilon$	10m, ..., 100m
$S_j$	260 seconds to 1 second
$\mathcal{N}$	300, ..., 3000
$\gamma_r$	0.2, ..., 1.2
$\eta$	6, ..., 600
$\gamma_c$	0.2, ..., 1.2
$\mathcal{M}$	500

of the most popular video content. The second set of simulations is conducted to study the performance of the BD2D approach by taking into account physical wireless network conditions such as interference, path loss and shadowing.

### A. FINDING THE OPTIMAL VALUES

We ignore the interference among all wireless nodes for this set of simulations. Next, we illustrate our basic simulation setup, then a detailed analysis on the achieved results is presented. The parameters and their corresponding values are given in Table 2.

#### 1) SIMULATION SETUP

Given the transmission radius  $\epsilon$ , first we distribute the BSNs in a square area of  $600 \times 600\text{-m}^2$  for different values of  $\lambda_\eta$  such that two neighboring BSNs can have an active D2D link with their corresponding receivers simultaneously.<sup>9</sup> For simplicity, we assume that the transmission range, i.e.,  $\epsilon$  of all wireless nodes in a cell is fixed. The transmission power of wireless nodes determines the number of D2D links that can be active in a cell simultaneously. This means that, the higher the transmission power of wireless nodes, the fewer D2D links that could be active in a cell [35]. We follow the proposed algorithm (see Fig. 2) to search for the BSNs that have cached the initial-segments of desired video content.

Each BSN will cache initial-segments of the unique video files.<sup>10</sup> We assume that each BSN can store only one Standard-Definition ( $640 \times 480$ ) YouTube video file at a rate of 24 frames per sec (fps) with 24 bit color depth due to its physical limitation. The size and number of initial-segments should not exceed the average length of the YouTube video file. According to one study, the average duration of the top YouTube video files is approximately 4 minutes and 20 seconds [43]. We varied the size of initial-segments i.e., from 5484 MB to 47 MB (or from 260 seconds to 1 second in duration) to observe the impact of size of initial-segments on average cache-hit ratio and average *startup-time*. The size of the initial-segment measures the corresponding number of video contents of which initial-segments will be cached in each BSN.

We implemented a BD2D caching proposal using the random caching policy [44], [45]. To do so, we assign the

<sup>9</sup>We apply the brute force search algorithm to generate the random and non-overlapping positions of BSNs in a cell [42].

<sup>10</sup>In our simulations, we make sure that each BSN is caching no duplicates of the initial-segments of the video contents.

initial-segments of video files to graphically distributed BSNs according to the Zipf distribution with exponent  $\gamma_c$  from a library of  $\mathcal{N} = 500$  distinct video files. We generated 500 requests for initial-segments from arbitrary positions in a cell, according to request distribution exponent  $\gamma_r = 0.6$ .<sup>11</sup> We compare the random BD2D caching approach with: the Most-Popular-Caching-Only (MPCO)<sup>12</sup> policy [48], when each BSN is caching the initial-segments of the most popular video files; and traditional D2D random caching [15], [16], [18], [20], when each BSN is caching a complete video file.

#### 2) EVALUATION METRIC

For the comparison of caching strategies the average cache-hit ratio (CHR) is used as the performance criterion and is computed using the equation given below [49]:

$$\text{CHR} = \left( \frac{\sum_i^{\mathcal{M}} \text{CacheHit}_i}{\sum_i^{\mathcal{M}} \text{CacheHit}_i + \sum_i^{\mathcal{M}} \text{CacheMiss}_i} \right) \times 100, \quad (14)$$

where  $\mathcal{M}$  is the number of requests<sup>13</sup> for the initial-segments of desired video files in a cell,  $\text{CacheHit}_i$  refers to the number of requests for the initial-segments satisfied within the vicinity of requested UEs, and  $\text{CacheMiss}_i$  refers to UEs' requests that are unable to find the initial-segments within their transmission range.

#### 3) SIMULATION RESULTS-I

Fig. 3 shows the average cache-hit ratio versus the size of the initial-segment for different values of the exponent of caching distribution  $\gamma_c$  when the number of BSNs  $\eta = 70$ ,<sup>14</sup> and cellular users are generating requests randomly for the initial-segments of video files with the request probability distribution  $\gamma_r = 0.6$ . We can observe from the figure that the average cache-hit ratio increases as the size of the initial-segments decreases. For instance, we can observe that, when each BSN is caching a complete video file (i.e., 260 seconds in duration), we get the average cache-hit ratio from 10% to 20% approximately for all values of  $\gamma_c$ . However, when the size of the initial-segment decreases, i.e., from 3 seconds to 1 second, the average cache-hit ratio rises to 100%. This indicates that, in comparison to caching a single large video chunk, caching only initial-segments creates a very large and diverse virtual pool of a cache of initial-segments (VCI) and users get the opportunity to find the initial-segments of desired video content within their vicinity. We can also observe from the figure that the average cache-hit ratio increases for all different values of  $\gamma_c$  as we decrease the

<sup>11</sup>This value has been evaluated in a measurement study conducted in 2008 on the University of Massachusetts Amherst campus [46].

<sup>12</sup>We selected the MPCO policy because according to one measurement study, the top 10% of the most popular videos account for up to 80% of the total videos on YouTube [47].

<sup>13</sup>Number of requests are equivalent to the number of UE<sub>i</sub> in the cell.

<sup>14</sup>The maximum number of BSNs that can be distributed in a cell without overlapping for transmission range 30 is 70.

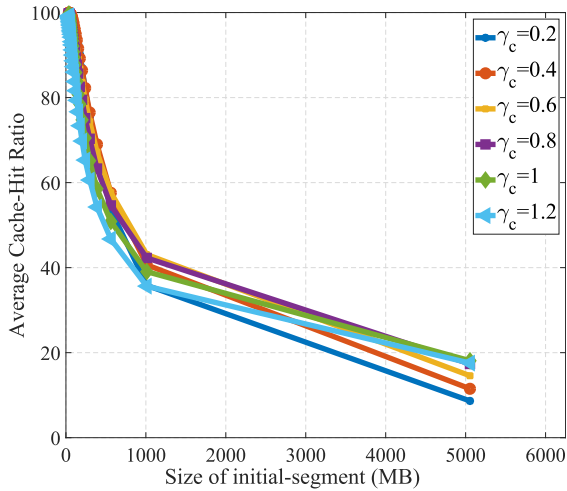


FIGURE 3. Average cache-hit ratio versus size of initial-segment for different values of  $\gamma_c$  with  $\epsilon_{max} = 30m$ ,  $\eta = 70$ ,  $\mathcal{N} = 500$  and  $\gamma_r = 0.6$ .

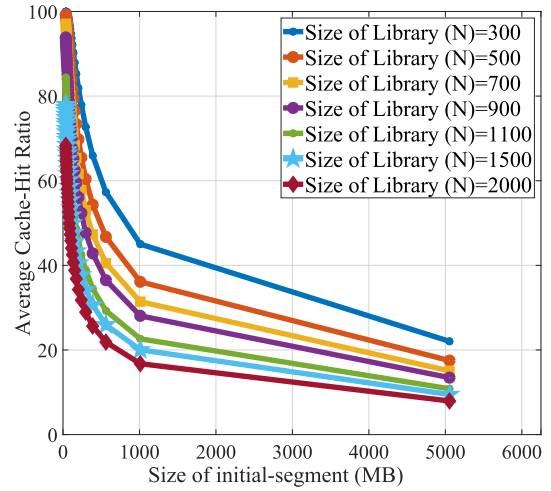


FIGURE 5. Average cache-hit ratio versus size of initial-segment for different library sizes  $\mathcal{N}$  with  $\gamma_{c,opt} = 1.2$ ,  $\eta = 70$ , and  $\gamma_r = 0.6$ .

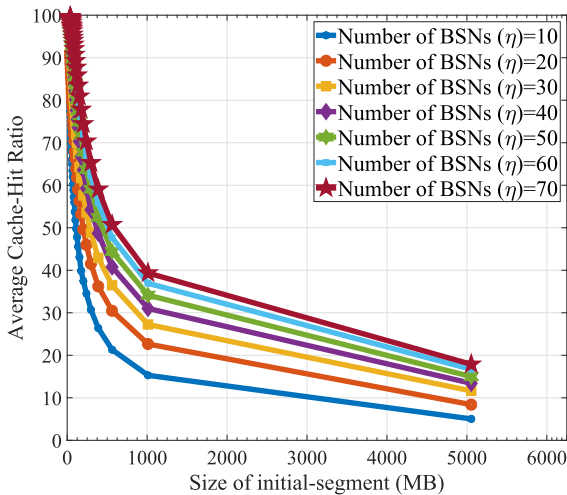


FIGURE 4. Average cache-hit ratio versus size of initial-segment for different number of BSNs ( $\eta$ ) with  $\gamma_{opt,c} = 1.2$ ,  $\gamma_r = 0.6$ , and  $\mathcal{N} = 500$ .

size of the initial-segment. However, initially, this increase is smaller for the large values of  $\gamma_c$ . This is because BSNs are caching the initial-segments of the most popular video files and users are requesting less popular files. But eventually large values of  $\gamma_c$  also attain the highest performance similar to other exponent values of cache distribution as the size of the initial-segment is decreased. This implies that a smaller initial-segment size adds randomness and dynamism to the VCI and users get the initial-segments of the most popular as well as least popular video files. Thus, we selected  $\gamma_c = 1.2$  as our optimal value of caching distribution and initial-segment size, i.e., 1 to 3 seconds in duration as our possible  $\mathcal{S}_{opt}$  values.

Fig. 4 shows how the density of BSNs in a cell affects the average cache-hit ratio for different sizes of initial-segments. We can observe that the percentage of the cache-hit ratio increases as the number of BSNs in a cell increases and the

size of the initial-segments decrease. The reason is that as we grow the population of BSNs in a cell, mobile users are not only surrounded by more and more neighboring BSNs, but the aggregated size of VCI also quickly increases in comparison to the cache of a single large video chunk or file. This provides a great opportunity for users to satisfy their random requests for initial-segments from a neighboring device at a short distance.

Fig. 5 shows the impact of size of the library on the average cache-hit ratio for different sizes of the initial-segments. We can observe from the figure that as the size of the library is increased the percentage of average cache-hit ratio decreases. The reason is obvious; an increase in size of the library also adds diversity and randomness to the video library. Now users can request initial-segments of more dynamic and random video content from the library. This means VCI should also be filled with initial-segments of more dynamic and random video files. Therefore, to satisfy the users' dynamic requests for initial-segments of video content, the number of BSNs and size of storage capacity should be increased.

Fig. 6 shows how different values of request distribution exponent, i.e.,  $\gamma_r$ , affects the average cache-hit ratio for  $\mathcal{S}_{opt} = 3$  seconds,  $\gamma_{c,opt} = 1.2$  and  $\eta = 70$ . It can be observed from the figure that for  $\gamma_{c,opt}$ , values of the  $\gamma_r$  has a very small effect on the average cache-hit ratio and the performance achieved is from 96% to 100%. The implication is that the optimal value of  $\gamma_c$  and  $\eta$  has created a very large and diverse virtual cache pool of initial-segments (VCI) of the most popular and least popular video files. Thus, users' requests for the initial-segments of desired and dynamic video content can be satisfied through the BD2D system without needing to go through the BS.

We have studied the effect of the transmission range  $\epsilon$  of mobile devices on the average cache-hit ratio in Fig. 7. The optimal initial-segment size, i.e.,  $\mathcal{S}_{opt}$  is 3 seconds. For a smooth and simultaneous multiple D2D transmissions,

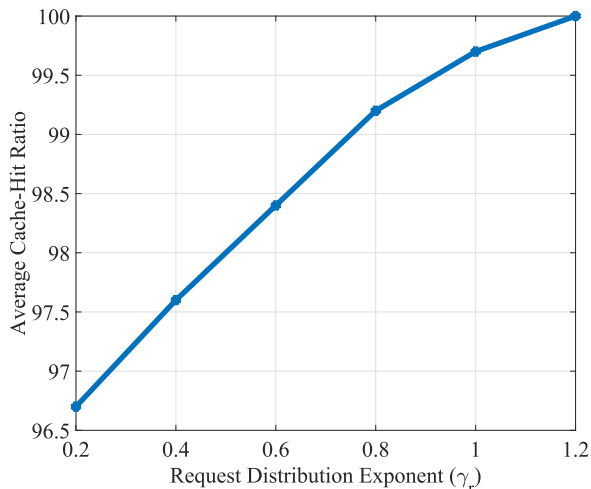


FIGURE 6. Effects of different values of request distribution exponent ( $\gamma_r$ ) on  $\gamma_{c,opt}$  for  $\eta = 70$ , and  $\mathcal{N} = 500$ .

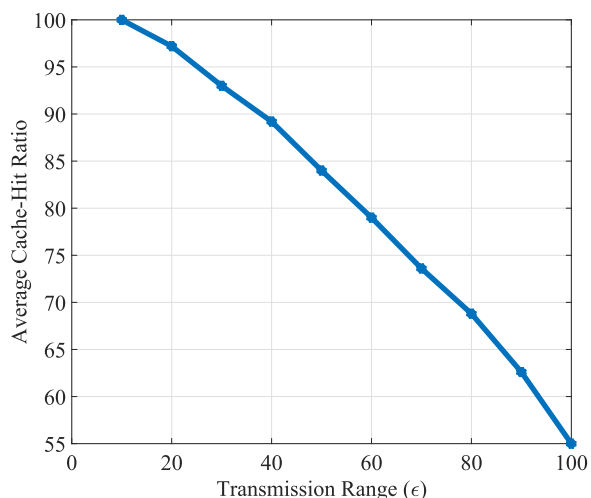


FIGURE 7. Average cache-hit ratio versus the transmission range ( $\epsilon$ ) with  $S_{opt} = 3$  seconds,  $\mathcal{N} = 500$ ,  $\gamma_{c,opt} = 1.2$ ,  $\gamma_r = 0.6$ .

we apply the brute force search algorithm for each value of  $\epsilon$  and deployed the maximum number of BSNs randomly without overlapping each other.<sup>15</sup> The small value of  $\epsilon$  means that a large number of BSNs can establish a D2D connection with their receivers simultaneously. For instance, for transmission range 10m we randomly deployed 600 BSNs in a cell. Whereas for transmission range 100m we could only deploy 6 BSNs randomly in a cell. We can observe that the average cache-hit ratio increases as we decrease the value of the transmission range  $\epsilon$ . The arguments for this figure are the same as we have described for Fig. 4. The transmission range and the resulting density of BSNs greatly impact the average cache-hit ratio. From transmission range 30m to 10m BD2D caching achieves its highest performance, i.e., from

<sup>15</sup>In contrast to a clustering approach in which devices within the clusters are allowed to have a D2D connection we used this non-overlapping technique to make the deployment of BSNs more general and realistic.

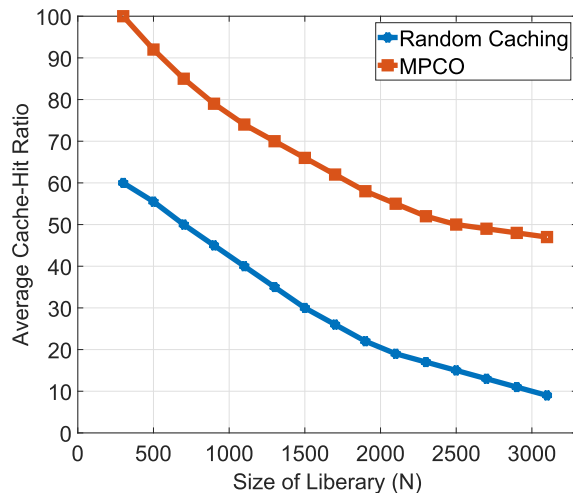


FIGURE 8. Comparison between random and MPCO techniques for different sizes of library  $\mathcal{N}$  when  $S_{opt} = 3$  seconds,  $\gamma_{c,opt} = 1.2$ ,  $\eta = 70$ , and  $\gamma_r = 0.6$ .

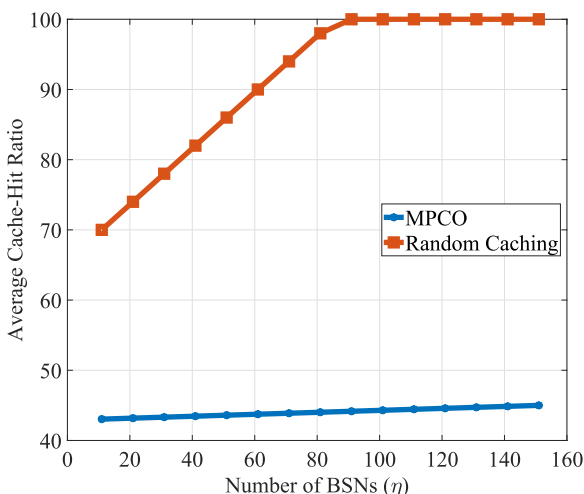


FIGURE 9. Comparison between random and MPCO techniques for different number of BSNs when  $S_{opt} = 3$  seconds,  $\gamma_{c,opt} = 1.2$ ,  $\eta = 70$ , and  $\gamma_r = 0.6$ .

90% to 100%. This means that users can download the initial-segments of desired video content from the BSNs at a very short range.

COMPARISON BETWEEN CACHING POLICIES (RANDOM BD2D AND MPCO)

Now, we compare the performance of random BD2D with the MPCO BD2D caching approach in Fig. 8, Fig. 9, Fig. 10 and Fig. 11. These figures illustrate that random caching shows better performance than MPCO. This is due to the fact that, in MPCO technique each BSN is caching the initial-segments of similar video content, which increases the number of redundant contents in VCI. Therefore, the chances of finding initial-segments of dynamic and random video content within the transmission range of requesting users are also lower in comparison to the random caching policy. Although in

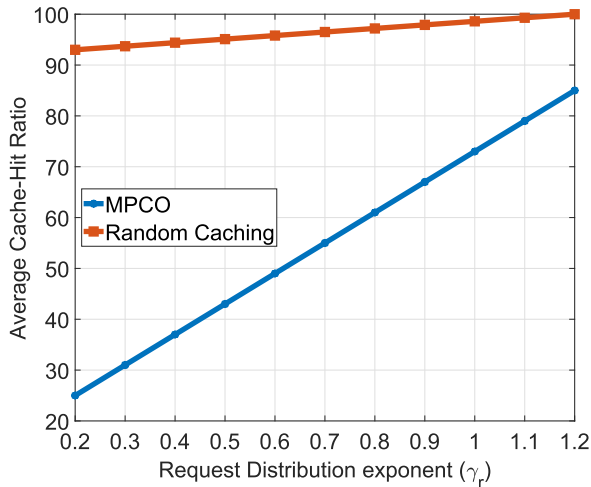


FIGURE 10. Comparison between random and MPCO techniques for different values of  $\gamma_r$ , when  $S_{opt} = 3$  seconds,  $\gamma_{c,opt} = 1.2$ , and  $\eta = 70$ .

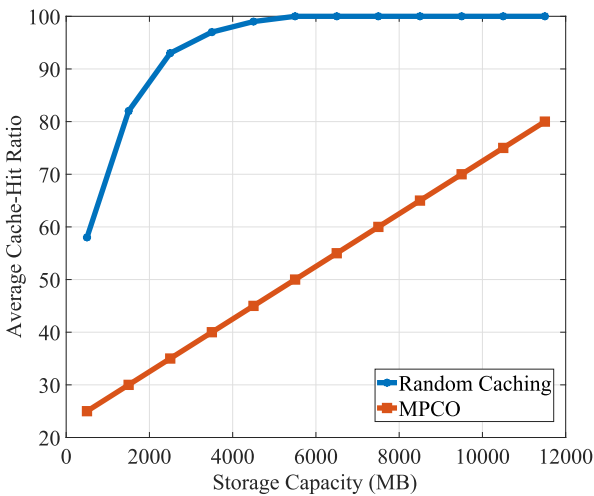


FIGURE 11. Comparison between random and MPCO techniques for different sizes of storage capacity  $C$  when  $S_{opt} = 3$  seconds,  $\gamma_{c,opt} = 1.2$ ,  $\eta = 70$ , and  $\gamma_r = 0.6$ .

random caching the cached initial-segments may overlap, due to the randomness and size of VCI the percentage of the average cache-hit ratio for random caching is higher than that for MPCO policy.

Fig. 8 shows the effects of the size of library on the average cache-hit ratio for random and MPCO. We can observe from the figure that the performance of both caching techniques worsens as we increase the size of the library but random caching performs better. The arguments for this behavior have already been discussed in Fig. 5 for random caching policy. In the case of MPCO, the obvious reason is the presence of redundant video contents in a VCI.

Fig. 9 compares the effects of the number of BSNs vs the average cache-hit ratio for random and MPCO. This figure illustrates that random caching outperforms as we grow the population of BSNs in a cell, whereas the performance and behavior of MPCO is very random. The reason is that,

since each BSN is caching similar content, an increase in population of BSNs also increases redundancy in contents stored in VCI. This decreases the probability of finding the initial-segments of users' requests for random and dynamic video content. Therefore, improvement in performance of MPCO is random and lower in comparison to a random caching policy.

Fig. 10 compares the performance of random and MPCO strategy for different values of  $\gamma_r$  on  $\gamma_{c,opt}$ . The effect of  $\gamma_r$  on  $\gamma_{c,opt}$  for random caching is the same as we discussed in Fig. 6. However, the performance of MPCO improves as we increase the value of  $\gamma_r$ . The reason is that, for the small value of  $\gamma_r$  the probability of finding the less popular files among a virtual cache pool of the most popular video files is much less. However, as we increase the value of  $\gamma_r$  the average cache-hit ratio also increases, which also increases the probability of finding the initial-segment of desired video content within the vicinity of requesting cellular user. The performance of MPCO is higher for a larger value of  $\gamma_r$  but poorer than a random caching policy.

Fig. 11 compares the effects of storage capacity on a cache-hit ratio between random and MPCO. We can observe from the figure that random caching shows a higher performance for small cache capacity in comparison to MPCO policy, which means mobile devices with small storage space can also contribute to a network in terms of reducing average startup-time.

In summary, a BD2D approach with a random caching policy has the capacity to satisfy the users' random and dynamic demands for initial-segments of desired video contents with a small storage space, few BSNs and at a very short distance, i.e., from 10m to 30m. In the next section we will investigate and discuss how different wireless network conditions such as interference and shadowing impact the startup-time when users download the initial-segments using the random BD2D caching approach.

### B. FINDING THE AVERAGE STARTUP-TIME

In this second set of simulation experiments, first we discuss the simulation environment, performance metrics and channel models for two types of communication, i.e., between D2D-link and device-to-BS link. Then, we discuss our simulation results in detail.

#### 1) DEPLOYMENT ENVIRONMENT

To evaluate the performance of BD2D in a realistic scenario, we consider the office environment for our simulation experiments. Specifically, we assume that our single cell consists of a Manhattan grid of square buildings of dimension 50m<sup>2</sup>. Each square plan building consists of offices, corridors and multiple floors. The size of each office is 6.2m<sup>2</sup>.

Our channel models for the cellular and D2D communication links are based on realistic assumptions. The former is based on a 4th generation cellular standard and the latter uses the 2.4 GHz D2D channel model. We take into account physical wireless network conditions such as interference,

TABLE 3. Simulation parameters of second set of simulations.

Parameters	Value
Building dimension	50m <sup>2</sup>
Office size	60m <sup>2</sup>
BS Height	25m
UE Height	1.5m
Floors	7
LOS	In the same room
NLOS	In different rooms or buildings
$B$ (Cellular transmission)	20MHz
$B$ (D2D transmission)	20MHz
$f_c$ (D2D Transmission)	2.1GHz
$f_c$ (Cellular Transmission)	2.45GHz
$P_{TX}$ (D2D Transmission)	20dBm
$P_{TX}$ (Cellular Transmission)	43dBm
$G_t$ (D2D Transmission)	12dBm
$G_t$ (Cellular Transmission)	12dBm
$G_r$ (D2D Transmission)	0
$G_r$ (Cellular Transmission)	0
$A1$ (LOS)	18.7
$A2$ (LOS)	46.8
$A3$ (LOS)	20
$A1$ (NLOS)	36.8
$A2$ (NLOS)	43.8
$A3$ (NLOS)	20
$12n_w$	Heavy wall loss parameter for $w=12$ (NLOS)
$5n_w$	light wall loss parameter for $n=7$ (NLOS)

path loss and shadowing.<sup>16</sup> All the simulation parameters are summarized in Table 3.

## 2) EVALUATION METRIC

We used the average *startup-time* as our performance metric which is obtained by taking a summation on an average *startup-time* of each user’s request that gets the opportunity to download the initial-segment of desired video content within the vicinity through a BD2D approach. Mathematically, it is given as  $\sum_{k \in \mathcal{R}} S_k$ ; where  $\mathcal{R}$  is the number of satisfied users’ requests. The *startup-time* of requested video files depends on many parameter values and is computed as:

$$S_{\mathcal{T}} = \mathcal{D}_{\mathcal{T}} + \mathcal{D}_{\mathcal{Q}} + \mathcal{D}_{\mathcal{P}} + \mathcal{D}_{\mathcal{L}} + \mathcal{D}_{\mathcal{C}}, \quad (15)$$

where  $\mathcal{D}_{\mathcal{T}}$  is the transmission time of an initial-segment from the transmitter to the requesting user,  $\mathcal{D}_{\mathcal{Q}}$  is the queuing delay which is defined as the total time taken when a mobile user requests for an initial-segment from the dTracker and receives the information of the BSN to establish a connection,  $\mathcal{D}_{\mathcal{P}}$  is the propagation delay,  $\mathcal{D}_{\mathcal{L}}$  indicates the playback delay which is the total time that a user waits to fill the buffer until there was smooth playback, and  $\mathcal{D}_{\mathcal{C}}$  is the total time taken by the pair of transmitters and receivers to establish a connection. For simplicity, we assume that  $\mathcal{D}_{\mathcal{Q}}$ ,  $\mathcal{D}_{\mathcal{L}}$ , and  $\mathcal{D}_{\mathcal{C}}$  are negligible or constant for all users’ requests.

The transmission time  $\mathcal{D}_{\mathcal{T}}$  depends on the size of an initial-segment of a requested content  $j$  i.e.  $S_j$  and the link rate  $\mathcal{L}_r$

<sup>16</sup>According to Golrezaei et al. [35], the effects of small scale fading can be reduced using the time scale of interest and frequency diversity over the bandwidth; therefore, we are not taking into account its effects in our simulation experiments.

between a pair of transmitters and receivers. The channel capacity of a communication link depends on the physical quantities such as transmission power, interference and path-loss. We computed the channel capacity of each communication link using the Shannon capacity formula:

$$\mathcal{L}_r = B \cdot \log_2(1 + SNIR), \quad (16)$$

where,  $B$  denotes the signal channel bandwidth, and SNIR is the Signal to Interference plus Noise Ratio and is given by:

$$SNIR = \frac{P_S}{P_N + P_I}, \quad (17)$$

$$P_S = P_{TX} + G_t + G_r - PL(\epsilon), \quad (18)$$

where  $P_{TX}$  is the transmission power of a transmitting,  $G_t$  indicates the transmit antenna gain,  $G_r$  indicates the received antenna gain,  $PL(\epsilon)$  represents the path loss model, and  $P_I$  is the sum of all interference at a receiver. The noise power on a dB scale is given by:

$$P_{N_{dB}} = 10 \log_{10}(k_B T_e) + 10 \log_{10} B + F_N, \quad (19)$$

where  $k_B T_e = 174 \text{ dBm/Hz}$  is the noise power spectral density and  $F_N = 6 \text{ dB}$  represents a noise figure of the receiving device.

## 3) CHANNEL MODEL

We use the WINNER II channel model (A1) for communication inside the building. We assume that all wireless nodes are inside the building and BS is outside the building. The path loss model for indoor communication (A1) for both Line-of-Sight (LOS) and Non-Line-of-Sight (NLOS) is given by:

$$PL = A1 \log_{10}(\epsilon) + A2 + A3 \log_{10}(f_c[\text{GHz}]/5) + X + \chi_\alpha + \sigma_{L_b}, \quad (20)$$

where  $f_c$ , indicates the carrier frequency.  $A1$  includes the path loss exponent.  $A2$  represents the intercept and  $A3$  shows the path loss frequency dependency.  $X = 5n_w$  is the (light) wall penetration parameter, where  $n_w$  is the number of walls between transmitter and receiver.  $\chi_\alpha$  indicates the shadowing parameter. Its value is assumed to be based on log-normal distribution with mean zero and standard deviation  $\sigma$ , where  $\sigma_{LOS} = 3$  and  $\sigma_{NLOS} = 6$ .  $\sigma_{L_b}$  is the body shadowing loss [32]. For LOS,  $\sigma_{L_b} = 4.2$  and for NLOS,  $\sigma_{L_b} = 3.6$ .

## 4) SIMULATION RESULTS-II

In Fig. 12, we investigate the effects of different sizes of initial-segments on the average *startup-time* for different numbers of BSNs when each BSN is caching initial-segments of video files according to  $\gamma_{c,opt} = 1.2$ . We can observe that in comparison to caching a large size initial-segment the average *startup-time* decreases as we start to deliver the video file in small size video chunks. For instance, for a segment size of 260 seconds, a higher average *startup-time* is achieved. However, as we decrease the size of the initial-segments e.g., from 3 seconds to 1 second, the BD2D approach achieves

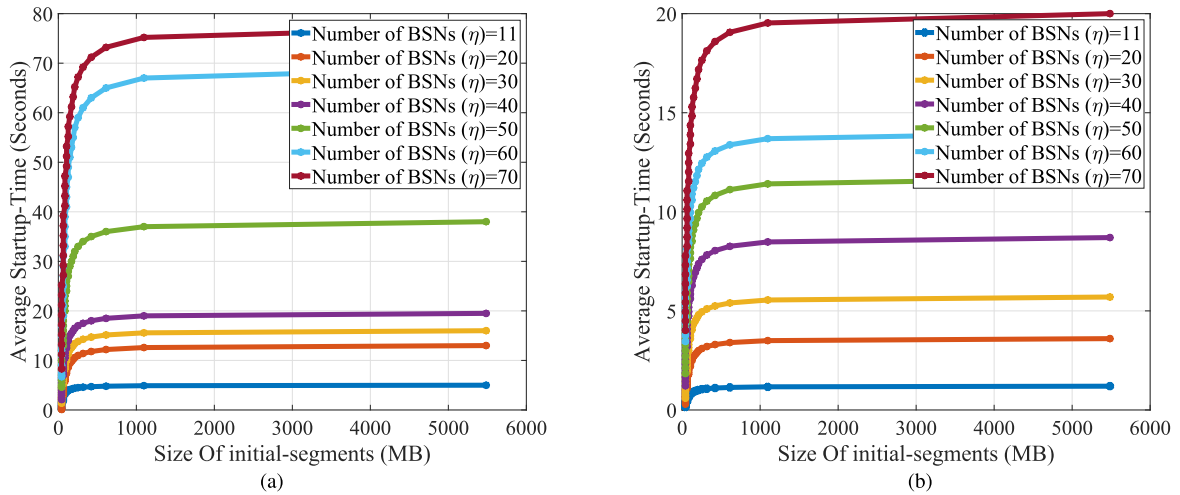


**FIGURE 12.** Impact of size of initial-segment versus the average *startup-time* for different number of BSNs with  $\gamma_{c,opt}$  and  $\gamma_r = 0.6$ . (a) Impact of size of the initial-segment on the average *startup-time* for LOS scenario. (b) Impact of the initial-segment size on the average *startup-time* for NLOS scenario.

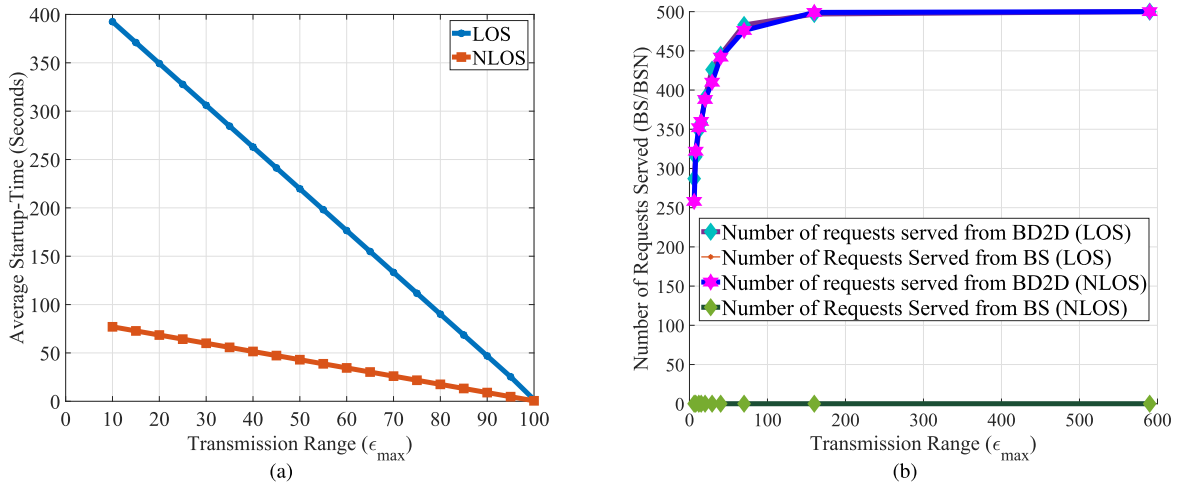


**FIGURE 13.** Comparison of performance of a BD2D system with the traditional cellular system for  $\eta_{opt}, \gamma_{c,opt} = 3$  seconds and  $\gamma_r = 0.6$  in terms of average *startup-time* and number of requests served from BS and BSNs respectively. (a) Performance of indoor LOS and NLOS scenario. (b) Performance of indoor LOS and NLOS scenario.

high performance in terms of minimum average *startup-time*. As we have discussed earlier, a smaller initial-segment size not only increases the probability of finding the initial-segments of the desired video files within the vicinity but also minimizes the average *startup-time* for the initial-video clips to be viewed by the wireless users due to the short distance between the transmitters and receivers. We can also observe from Fig. 12 that the average *startup-time* increases as we increase the population of BSNs in a cell. The impact of the number of BSNs on the average *startup-time* is twofold. On the one hand, a higher number of BSNs allows users to download the initial-segments using a D2D link. On the other hand, the existence of multiple D2D connections increases the sum of interference at each receiver, which impacts the channel quality and in turn reduces the data rate. From the figure we can also observe the behavior of LOS and NLOS

scenarios for the indoor office model. The performance of NLOS in terms of achieving a lower average *startup-time* is better than the LOS. The reason is that, due to NLOS interference there is a probability that there exists on average less interference at each receiving node. Hence, as the sum of the interference at receivers decreases, consequently the channel rate increases.

Fig. 13 shows the impact of the transmission range of wireless users on average *startup-time*. It can be observed from the figure that average *startup-time* is higher for the smallest value of  $\epsilon$  (i.e.,  $\epsilon = 10m, \eta = 600$ ) and starts to reduce as the transmission range is increased. The effect of transmission range on average *startup-time* is twofold. On the one hand, a smaller transmission range allows the deployment of a large number of BSNs in a cell; consequently the chances of finding the initial-segments of the desired video content at

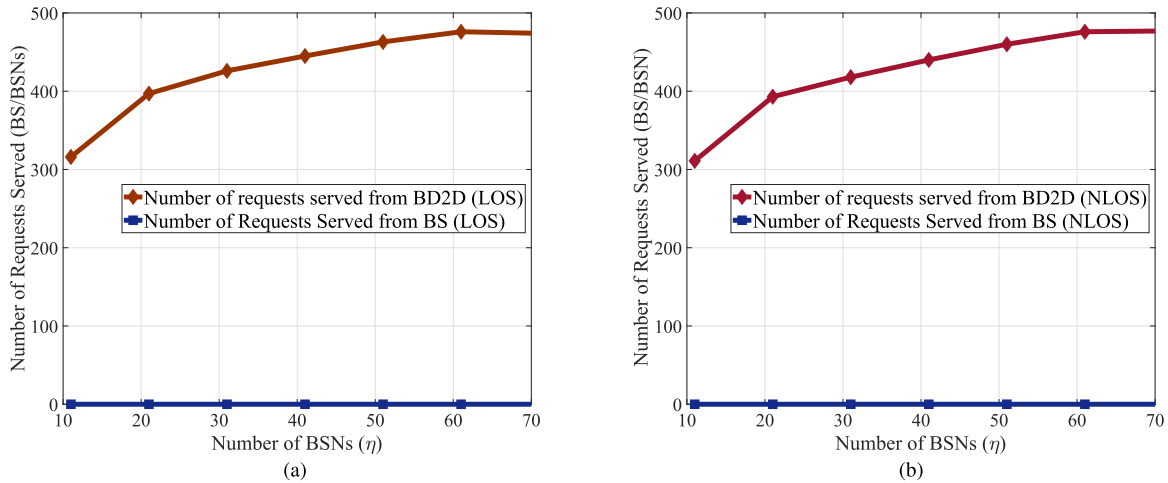


**FIGURE 14.** Comparison of performance of a BD2D system with the traditional cellular system for  $\eta_{opt}, \gamma_{c,opt} = 3$  seconds and  $\gamma_r = 0.6$ . (a) Performance of indoor LOS scenario. (b) Performance of indoor NLOS scenario.

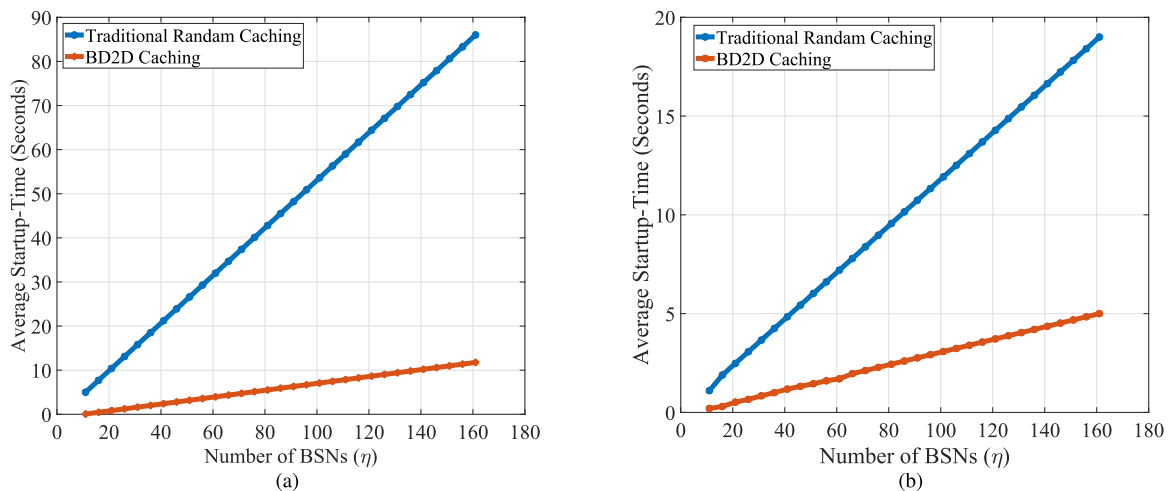


**FIGURE 15.** Comparison of performance of a BD2D system with the traditional caching system (LOS and NLOS scenario) for  $\gamma_{c,opt} = 1.2$ ,  $S_{opt} = 3$  seconds,  $\gamma_r = 0.6$ , and  $\eta = 160$  to 10 in terms of average *startup-time*. (a) Performance of indoor LOS. (b) Performance of indoor NLOS scenario.

a very short distance are also much higher. On the other hand, higher density of BSNs increases the number of transmitters which in turn increases the probability of having higher LOS interference at each receiving device. This can degrade the performance of a BD2D system. However, from the figure we also conclude that downloading the initial-segments from a short range distance device yields a better performance than downloading through the BS; even in the presence of multiple transmitters and with resulting higher interference power.

Fig. 14 shows the results for mode selection or number of requests served from a BD2D system and pure cellular system (i.e., from the BS). The mode is selected on the basis of channel quality of the D2D-link and the Device-BS link once the initial-segment has been found within the transmission range of a requesting user. Here in this experiment, we assume that the base station resides 100m from each device and

each BSN is caching the initial-segments according to  $S_{opt}$  and  $\gamma_{c,opt}$ . The transmission range of each cellular user is 20m and a number of BSNs, i.e.,  $\eta = 70$ . We can observe that a BD2D system markedly outperforms the cellular system in terms of delivering initial video clips with a minimum *startup-time*. Although the presence of multiple D2D pairs and other wireless network conditions add interference at each receiving device and are the most important aspects to consider, the availability of an initial-segment within the short distance and the corresponding higher channel capacity also play a very significant role. This allows D2D technology to become a very suitable candidate in providing minimum *startup-time* for short length video viewers in a cellular network.

In Fig. 15, we compare the performance of the traditional random caching system [35] with the BD2D caching system in terms of average *startup-time*. In the traditional caching

system each BSN is caching the complete video file according to  $\gamma_{c,opt} = 1.2$ . In the BD2D system each BSN is caching the initial-segments of the video files according to  $\gamma_{c,opt} = 1.2$  and  $\mathcal{S}_{opt} = 3$  seconds. The transmission range of each user is 10m and the number of BSNs varies from 160 to 10. We can observe from the figure that a BD2D system performs better than the traditional caching system in terms of delivering the initial video clips with a minimum *startup-time*. The reason is that, the aggregated size of VCI in a BD2D system is larger than the size of VCI in a traditional caching system. This increases opportunities for wireless users to find and download the initial-segments of the desired video files from a neighboring device at a very short distance with minimum *startup-time*. From the figure we can also observe that, the performance of NLOS in terms of achieving lower average *startup-time* is better than the LOS. As we have already discussed in Fig. 12 that, due to NLOS interference there exists on average less interference at each receiving node which consequently increases the channel rate.

## V. CONCLUSION

In this paper, we propose a BD2D caching approach in which D2D devices randomly cache the initial-segments of the most popular video content and share with the devices in close proximity using a D2D direct link. We also introduced a new network-assisted D2D architecture called a M-BD2D system that assists the mobile devices in discovering the BSNs, in cache placement decisions, and in registration at the core network. The M-BD2D system uses servers deployed within the SGWs as a centralized *Tracker-server* to manage and collect the cache and location related information of the BSNs.

Our simulation experiments have shown that, typical wireless network conditions such as interference and shadowing may impact the performance of a BD2D approach. However, a BD2D system with a simple random caching approach works better in comparison to the traditional cellular communication system. The mobility support in terms of cache-exchange-information, when a BSN moves from one eNodeB to another eNodeB, is not considered in this paper and is one of the most important future directions to explore. In practice, users are unwilling to share their data over the D2D link due to limited energy and storage resources. There is a need for economically sound incentive mechanisms to encourage user participation and is a promising direction for future research. Furthermore, the performance of a BD2D system can be evaluated using the available real-world data and may be considered as a most interesting direction of work in the future.

## REFERENCES

- [1] Cisco. (Feb. 2017). *Cisco Visual Networking Index: Global Mobile Data Traffic Forecast Update, 2016–2021*. [Online]. Available: <https://www.akamai.com/cn/zh/multimedia/documents/white-paper/maximizing-audience-engagement-white-paper.pdf>
- [2] S. S. Krishnan and R. K. Sitaraman, "Video stream quality impacts viewer behavior: Inferring causality using quasi-experimental designs," *IEEE/ACM Trans. Netw.*, vol. 21, no. 6, pp. 2001–2014, Dec. 2013.
- [3] "Maximizing audience engagement: How online video performance impacts viewer behavior," Akamai, Cambridge, MA, USA, White Paper, Jan. 2015. [Online]. Available: <https://www.cisco.com/c/en/us/solutions/collateral/service-provider/visual-networking-index-vni/mobile-white-paper-c11-520862.pdf>
- [4] N. Panwar, S. Sharma, and A. K. Singh, "A survey on 5G: The next generation of mobile communication," *Phys. Commun.*, vol. 18, pp. 64–84, Mar. 2016.
- [5] T. Salam, W. Rehman, and X. Tao, "Cooperative MTC data offloading with trust transitivity framework in 5G networks," in *Proc. IEEE Global Commun. Conf. (GLOBECOM)*, Dec. 2017, pp. 1–7.
- [6] A. Shadmand and M. Shikh-Bahaei, "Multi-user time-frequency down-link scheduling and resource allocation for LTE cellular systems," in *Proc. IEEE Wireless Commun. Netw. Conf. (WCNC)*, Apr. 2010, pp. 1–6.
- [7] H. Saki and M. Shikh-Bahaei, "Cross-layer resource allocation for video streaming over OFDMA cognitive radio networks," *IEEE Trans. Multimedia*, vol. 17, no. 3, pp. 333–345, Mar. 2015.
- [8] M. M. Mahyari, A. Shojaefard, and M. Shikh-Bahaei, "Probabilistic radio resource allocation over CDMA-based cognitive radio networks," *IEEE Trans. Veh. Technol.*, vol. 64, no. 8, pp. 3560–3565, Aug. 2015.
- [9] M. Naslcheraghi, S. A. Ghorashi, and M. Shikh-Bahaei, "FD device-to-device communication for wireless video distribution," *IET Commun.*, vol. 11, no. 7, pp. 1074–1081, May 2017.
- [10] A. Shadmand, K. Nehra, and M. Shikh-Bahaei, "Cross-layer design in dynamic spectrum sharing systems," *EURASIP J. Wireless Commun. Netw.*, vol. 2010, Feb. 2010, Art. no. 458472.
- [11] H. Bobarshad and M. Shikh-Bahaei, "M/M/1 queuing model for adaptive cross-layer error protection in WLANs," in *Proc. IEEE Wireless Commun. Netw. Conf. (WCNC)*, Apr. 2009, pp. 1–6.
- [12] D. Astely, E. Dahlman, G. Fodor, S. Parkvall, and J. Sachs, "LTE release 12 and beyond [accepted from open call]," *IEEE Commun. Mag.*, vol. 51, no. 7, pp. 154–160, Jul. 2013.
- [13] X. Chen, J. Wu, Y. Cai, H. Zhang, and T. Chen, "Energy-efficiency oriented traffic offloading in wireless networks: A brief survey and a learning approach for heterogeneous cellular networks," *IEEE J. Sel. Areas Commun.*, vol. 33, no. 4, pp. 627–640, Apr. 2015.
- [14] A. Checko et al., "Cloud RAN for mobile networks—A technology overview," *IEEE Commun. Surveys Tuts.*, vol. 17, no. 1, pp. 405–426, 1st Quart., 2015.
- [15] T. Salam, W. Rehman, X. Tao, Y. Chen, and P. Zhang, "A trust framework based smart aggregation for machine type communication," *Sci. China Inf. Sci.*, vol. 60, no. 10, p. 100306, 2017.
- [16] X. Wang, Y. Zhang, V. C. M. Leung, N. Guizani, and T. Jiang, "D2D big data: Content deliveries over wireless device-to-device sharing in large-scale mobile networks," *IEEE Wireless Commun.*, vol. 25, no. 1, pp. 32–38, Feb. 2018.
- [17] M. Ji, G. Caire, and A. F. Molisch, "Fundamental limits of caching in wireless D2D networks," *IEEE Trans. Inf. Theory*, vol. 62, no. 2, pp. 849–869, Feb. 2016.
- [18] N. Golrezaei, A. G. Dimakis, and A. F. Molisch, "Scaling behavior for device-to-device communications with distributed caching," *IEEE Trans. Inf. Theory*, vol. 60, no. 7, pp. 4286–4298, Jul. 2014.
- [19] Y. Zhang, E. Pan, L. Song, W. Saad, Z. Dawy, and Z. Han, "Social network aware device-to-device communication in wireless networks," *IEEE Trans. Wireless Commun.*, vol. 14, no. 1, pp. 177–190, Jan. 2015.
- [20] D. Malak, M. Al-Shalash, and J. G. Andrews, "Optimizing content caching to maximize the density of successful receptions in device-to-device networking," *IEEE Trans. Commun.*, vol. 64, no. 10, pp. 4365–4380, Oct. 2016.
- [21] L. Zhang, M. Xiao, G. Wu, and S. Li, "Efficient scheduling and power allocation for d2d-assisted wireless caching networks," *IEEE J. Sel. Areas Commun.*, vol. 64, no. 6, pp. 2438–2452, Jun. 2016.
- [22] S. Krishnan and H. S. Dhillon, "Effect of user mobility on the performance of device-to-device networks with distributed caching," *IEEE Wireless Commun. Lett.*, vol. 6, no. 2, pp. 194–197, Apr. 2017.
- [23] N. Anjum, D. Karamshuk, M. Shikh-Bahaei, and N. Sastry, "Survey on peer-assisted content delivery networks," *Comput. Netw.*, vol. 116, pp. 79–95, Apr. 2017.



- [24] N. Anjum and M. Shikh-Bahaei. (2017). "Evaluation of availability of initial-segments of video files in device-to-device (D2D) network." [Online]. Available: <https://arxiv.org/abs/1710.07083>
- [25] K. Doppler, M. Rinne, C. Wijting, C. B. Ribeiro, and K. Hugl, "Device-to-device communication as an underlay to LTE-advanced networks," *IEEE Commun. Mag.*, vol. 47, no. 12, pp. 42–49, Dec. 2009.
- [26] M. J. Yang, S. Y. Lim, H. J. Park, and N. H. Park, "Solving the data overload: Device-to-device bearer control architecture for cellular data offloading," *IEEE Veh. Technol. Mag.*, vol. 8, no. 1, pp. 31–39, Mar. 2013.
- [27] R. Agarwal, V. Gauthier, M. Becker, T. Toukabrignes, and H. Afifi, "Large scale model for information dissemination with device to device communication using call details records," *Comput. Commun.*, vol. 59, pp. 1–11, Mar. 2015.
- [28] B. Raghthaman, E. Deng, R. Pragada, G. Sternberg, T. Deng, and K. Vanganuru, "Architecture and protocols for LTE-based device to device communication," in *Proc. Int. Conf. Comput., Netw. Commun. (ICNC)*, Jan. 2013, pp. 895–899.
- [29] A. Pyattaev, K. Johnsson, A. Surak, R. Florea, S. Andreev, and Y. Koucheryavy, "Network-assisted D2D communications: Implementing a technology prototype for cellular traffic offloading," in *Proc. IEEE Wireless Commun. Netw. Conf. (WCNC)*, Apr. 2014, pp. 3266–3271.
- [30] J. He, H. Zhang, B. Zhao, and S. Rangarajan. (2014). "A collaborative framework for in-network video caching in mobile networks." [Online]. Available: <https://arxiv.org/abs/1404.1108>
- [31] J. He and W. Song, "Optimizing video request routing in mobile networks with built-in content caching," *IEEE Trans. Mobile Comput.*, vol. 15, no. 7, pp. 1714–1727, Jul. 2016.
- [32] M. Ji, G. Caire, and A. F. Molisch, "Wireless device-to-device caching networks: Basic principles and system performance," *IEEE J. Sel. Areas Commun.*, vol. 34, no. 1, pp. 176–189, Jan. 2016.
- [33] (Aug. 2017). *Winner II Channel Models*. [Online]. Available: <https://cept.org/files/8339/winner.pdf>
- [34] Y. Li, Y. Zhang, and R. Yuan, "Measurement and analysis of a large scale commercial mobile Internet TV system," in *Proc. ACM SIGCOMM Conf. Internet Meas. Conf.*, 2011, pp. 209–224.
- [35] N. Golrezaei, P. Mansourifard, A. F. Molisch, and A. G. Dimakis, "Base-station assisted device-to-device communications for high-throughput wireless video networks," *IEEE Trans. Wireless Commun.*, vol. 13, no. 7, pp. 3665–3676, Jul. 2014.
- [36] X. Wang, M. Chen, T. Taleb, A. Ksentini, and V. C. M. Leung, "Cache in the air: Exploiting content caching and delivery techniques for 5G systems," *IEEE Commun. Mag.*, vol. 52, no. 2, pp. 131–139, Feb. 2014.
- [37] P. Phunchongharn, E. Hossain, and D. I. Kim, "Resource allocation for device-to-device communications underlying LTE-advanced networks," *IEEE Wireless Commun.*, vol. 20, no. 4, pp. 91–100, Aug. 2013.
- [38] A. Asadi, Q. Wang, and V. Mancuso, "A survey on device-to-device communication in cellular networks," *IEEE Commun. Surveys Tuts.*, vol. 16, no. 4, pp. 1801–1819, 4th Quart., 2014.
- [39] M. Liebsch and F. Z. Yousaf, "Runtime relocation of CDN serving points-enabler for low costs mobile content delivery," in *Proc. IEEE Wireless Commun. Netw. Conf. (WCNC)*, Apr. 2013, pp. 1464–1469.
- [40] T. T. Gunes and H. Afifi, "Hybrid model for LTE network-assisted D2D communications," in *Proc. Int. Conf. Ad-Hoc Netw. Wireless*. New York, NY, USA: Springer, Jun. 2014, pp. 100–113.
- [41] K. Doppler, C.-H. Yu, C. B. Ribeiro, and P. Janis, "Mode selection for device-to-device communication underlying an LTE-advanced network," in *Proc. IEEE Wireless Commun. Netw. Conf.*, Apr. 2010, pp. 1–6.
- [42] *Non Overlapping Randomly Located Circles*. Accessed: Jun. 1, 2018. [Online]. Available: <https://stackoverflow.com/questions/36177195/non-overlapping-randomly-located-circles>
- [43] Press Release. (Feb. 2014). *Comscore Releases January 2014 U.S. Online Video Rankings*. [Online]. Available: <http://www.comscore.com/Insights/Press-Releases/2014/2/comScore-Releases-January-2014-US-Online-Video-Rankings>
- [44] L. Zhou, D. Wu, J. Chen, and Z. Dong, "Greening the smart cities: Energy-efficient massive content delivery via D2D communications," *IEEE Trans. Inf. Format.*, vol. 14, no. 4, pp. 1626–1634, Apr. 2018.
- [45] M.-C. Lee, M. Ji, A. F. Molisch, and N. Sastry. (2018). "Performance of caching-based D2D video distribution with measured popularity distributions." [Online]. Available: <https://arxiv.org/abs/1806.05380>
- [46] *UMASS Trace Repository*. Accessed: Aug. 1, 2018. [Online]. Available: <http://traces.cs.umass.edu/index.php/Network/Network>
- [47] M. Cha, H. Kwak, P. Rodriguez, Y.-Y. Ahn, and S. Moon, "Analyzing the video popularity characteristics of large-scale user generated content systems," *IEEE/ACM Trans. Netw.*, vol. 17, no. 5, pp. 1357–1370, Oct. 2009.
- [48] Z. Chen, N. Pappas, and M. Kountouris, "Probabilistic caching in wireless D2D networks: Cache hit optimal versus throughput optimal," *IEEE Commun. Lett.*, vol. 21, no. 3, pp. 584–587, Mar. 2017.
- [49] C. Bernardini, T. Silverston, and O. Fester, "A comparison of caching strategies for content centric networking," in *Proc. IEEE Global Commun. Conf. (GLOBECOM)*, Dec. 2015, pp. 1–6.



**NASREEN ANJUM** received the M.S. (CS) degree in computer science from the City University of Science and Information Technology, Peshawar. She is currently pursuing the Ph.D. degree with the Department of Informatics, King's College London. She has been with the Shaheed Benazir Bhutto Women University, Peshawar, since 2007, as a Lecturer in computer science. Her research interests include CDN, mobile-CDN, P2P, device-to-device networks, and machine-to-machine communication. She was a recipient of the Fellowship Award, in 2014, 2015, 2016, and 2017, from the Schlumberger Faculty for the Future Fellowship Award.



**ZHAOHUI YANG** received the B.S. degree in information science and engineering from Chien-Shiung Wu Honors College, Southeast University, Nanjing, China, in 2014, and the Ph.D. degree in communication and information system from the National Mobile Communications Research Laboratory, Southeast University, in 2018. He is currently a Postdoctoral Research Associate with the Center for Telecommunications Research, Department of Informatics, King's College London, U.K. His research interests include full-duplex, UAV, URLLC, the IoT, edge computing, energy harvesting, and non-orthogonal multiple access. He was a TPC Member of the IEEE ICC, during 2015–2018, and GLOBECOM, during 2017–2018.



**HADI SAKI** received the Ph.D. degree in telecommunications from King's College London, U.K., in 2014, where he is currently a Research Fellow with the Department of Informatics, Faculty of Natural and Mathematical Sciences. His research interests include multimedia communications application in healthcare, radio resource allocation algorithms, cross-layer design and optimization, spectrum coexistence and cognitive radio, green heterogeneous networks, and latency aspects of mobile radio communications and IoT/M2M systems. He served as the Technical Program Chair of the Annual IEEE International Conference on Wireless Advanced, in 2018.



has also received the Best Teacher Award from the Army Degree College of Women, Peshawar.

**MEHREEN KIRAN** received the B.S. (CS) degree from the University of Peshawar, Pakistan, and the M.S. (CS) degree from the Institute of Management Sciences, Peshawar, in 2018. She was a Lecturer with the Army College of Education for Women. Her research interests include machine-to-machine and the IoT. She has achieved the gold medal in M.S. (CS). She has also received the Best Performance Award from the University of Peshawar for attaining good academic record. She



awarded three U.S. patents as an Inventor and as a Co-Inventor, respectively. In 2002, he joined King's College London as a Lecturer, where he is currently a Professor with the Centre for Telecommunications Research, Department of Informatics. He has authored or co-authored numerous journal and conference articles. He has been engaged in research in the area of wireless communications and signal processing for 25 years both in academic and industrial organizations. His research interests include resource allocation in full-duplex and cognitive dense networks, visual data communications over the IoT, applications in healthcare, and communication protocols for autonomous vehicle/drone networks. He is a Fellow of the IET and the Founder and the Chair of the Wireless Advanced Annual International Conference, from 2003 to 2012.

**MOHAMMAD SHIKH-BAHAEI** received the B.Sc. degree from the University of Tehran, Tehran, Iran, in 1992, the M.Sc. degree from the Sharif University of Technology, Tehran, in 1994, and the Ph.D. degree from King's College London, U.K., in 2000. He was with two start-up companies and with National Semiconductor Corp., Santa Clara, CA, USA (now part of Texas Instruments Incorporated), on the design of third generation (3G) mobile handsets, for which he has been

• • •